Inputs from in situ experiments to the understanding of the unsaturated behaviour of Callovo-Oxfordian claystone

Gilles Armand[1,a], Hippolyte Djizanne[1] , Jad Zghondi[1], Rémi de La Vaissière[1], Jean Talandier[2] and Nathalie Conil[1]

[1]*Andra, R&D Division, Meuse/Haute-Marne Underground Research Laboratory, 52290, Bure, France*
[2]*Andra, R&D Division, 1-7 rue Jean Monnet, 92290, Chatenay-Malabry, France*

Abstract. The French national radioactive waste management agency (Andra) research program is dedicated to preparing the construction and operation of a deep geological disposal facility for high-level and intermediate-level long-lived radioactive waste (HL, IL-LLW) in the Callovo-Oxfordian claystone (COx). The characterization of the COx thermo-hydro-mechanical (THM) behavior, at different scales of interest, must gradually give relevant data for design and safety calculations. The effects of saturation and desaturation of COx claystone are studied in laboratory conditions (sample scale) and in situ (drift scale), in order to improve knowledge on ventilation effect at gallery wall as galleries will remains open during operational phase (more than 100 years for some specific galleries) in the repository. The Saturation Damaged Zone (SDZ) experiment is outlined and its results are discussed. This experimentation aims to change the relative humidity in an isolated portion of a gallery in order to follow the HM behavior of the surrounding rock mass. Drying and wetting cycles could induce in certain cases cracks and swelling and modify the hydromechanical behavior of the claystone around the gallery (Young modulus, strength, creep…). The long term behavior of the COx claystone at the vicinity of gallery is then studied by performing climatic, hydraulic, geological and geomechanical measurements. Results of the in situ experiment are discussed with respect to the identified process on samples. The discussion given on this paper intends to highlights the inputs from 7 years of an in situ experiment to better understand the unsaturated behavior of the COx claystone.

1 Introduction

Clay formations in their natural state exhibit very favorable conditions for repository of radioactive waste, as they generally have a very low hydraulic conductivity, small molecular diffusion and significant retention capacity for radionuclide. Nevertheless, one concern regarding waste disposal is that, due to the necessary underground excavations and the associated disturbance and damage in the area close to these excavations, the favorable properties of such formations could change and the host rock could lose part of its barrier function and thus negatively influence the performance of a repository. That is why, in order to demonstrate feasibility of a radioactive waste repository in a claystone formation, the French national radioactive waste management agency (Andra) started in 2000 to build the Meuse/Haute-Marne underground research laboratory (URL) at Bure (at nearly 300 km East of Paris). The host formation consists of a Callovo-Oxfordian claystone (COx) laying between 420 m and 550 m depth, which is overlain and underlain by poorly permeable carbonate formations.

First, the main objective of the research was to characterize the confining properties of the clay through in situ hydrogeological tests, chemical measurements and diffusion experiments and to demonstrate that the construction and operation of a geological disposal will not introduce pathways for radionuclides migration [1]. The excavation worksite in the host layer is a scientific experimentation in itself to characterize the impacts of digging, to understand the hydro mechanical behaviour of the claystone and to study the excavated damaged zone (EDZ).

In France, the repository, if it will be allowed, will be operated during at least 100 years after it commissioning. Some of the drift will remain opened over a long period during which ventilation will activate. Then the effect of ventilation on rock mass behaviour around drift has to be understood, in particular to evaluate effect of ventilation over excavation damaged zone (EDZ). One of the experiments, called Saturation Damaged Zone (SDZ), is dedicated to the understanding of change of relative humidity over the drift behaviour and the excavation damaged zone (extent and permeability measurement).

It is known that drying test on clay soil leads to the fracturing of the clay. On claystone, fractures associated with the desaturation of argillaceous medium have been observed on gallery fronts in several underground research laboratories, e.g., in Tournemire [2] and Mont Terri underground research laboratory. Hedan et al [3] demonstrated the ability of the Digital image correlation

[a] Corresponding author: gilles.armand@andra.fr

(DIC) technique, to achieve a full displacement field measurement in order to monitor opening and closure of crack under climatic conditions changes at Tournemire URL. They show that cracks opening/closure are clearly correlated to changes in RH and T. Strains concentrate into narrow zones or bands indicating typical strain localization as also observed in the laboratory on samples. These narrow zones or bands were desiccation cracks (typical aperture 0.5 mm) that were observable from the displacement fields. The strain fields between these desiccation cracks were homogeneous at the spatial resolution used in this study. The hydric strains were anisotropic with larger strains perpendicular to desiccation cracks than those parallel to the same cracks. As observed at the Mont-Terri site, desiccation cracks close in summer and open in winter. However, contrary to the measurements acquired at the Swiss site, the crack apertures of the desiccation cracks were reversible after one year of data acquisition. Such annual climatic changes with high relative humidity in summer are not as severe at the Meuse/Haute-Marne URL due to the fact that accesses to the lab are through shafts with control ventilation.

At the main level of the Meuse/Haute-Marne URL, Armand et al [4] show that excavation works induce an important fracture pattern (shear an extension fractures) whose extent depends on the drift orientation versus the in situ principal stresses. The effect of relative humidity change on the behavior of the excavation induced fractures network is key point of SDZ experiment.

This paper first recalls some of the results of drying test performed on sample in order to investigate the desaturation effect on hydro mechanical behavior of the COx claystone. The major part of this paper is devoted to the description of SDZ experiment and results.

2 Callovo-oxfordian claystone

2.1 Mineralogy

Sediments of the Callovo–Oxfordian unit consist of a dominant clay fraction associated with carbonate, quartz with minor feldspars, and accessory minerals [5]. At the MHM URL main level (-490 m depth), the clay fraction is high (40–60%), and clay minerals consist of illite, ordered illite/smectite mixed layers, kaolinite, tri-octahedral, iron-rich chlorite, and minor biotite.

The Callovo–Oxfordian clay-rich rock porosity lies between 14% and 20% at the MHM URL site and is close to 18% at the URL main level [6], and natural water content ranges between 5% and 8%.

2.2 Microstructure

At the URL level, Callovo-Oxfordian claystone could be considered as a clay matrix (between 40 to 60% clay content) with inclusions of carbonate and tectosilicates grains. Those grains are rigid (regarding to clay matrix), not porous and their sizes are in a range of 0.1 to 100µm. As a consequence, most of the porosity is located in the clay matrix [7], and there is a correlation between clay content and porosity at the scale of Callovo-Oxfordian geological layer. Performed investigations to characterize this porosity indicate that pore network is composed mainly of meso/micro pores and shows a very low connectivity for pores over 40 nm [8]. Using various imaging techniques such as electron microscopy or Xray tomography mineral maps have been obtained [9] highlighting a preferential orientation parallel to the bedding of carbonate and tectosilicates inclusions (Figure 1). Nevertheless, orientation of clay particles and aggregates with the bedding plan is not too marked as it could be found in other indurated clays such as Opalinus Clay in Switzerland. This leads to a slight anisotropy in most properties of the rock especially in terms of solute diffusion or water permeability.

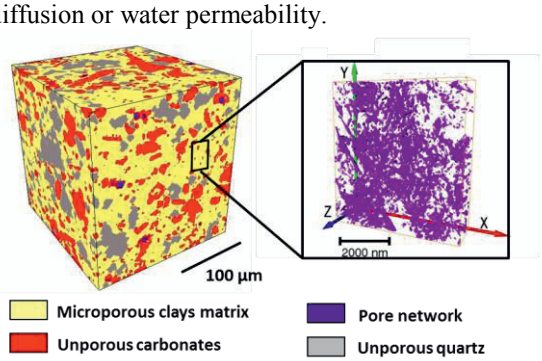

Figure 1. View of the microstruture of COx at different scales (a) clay matrix with carbonate and quartz inclusions [8], (b) pore network obtained by FIB/SEM methods [9].

3 Effect of desaturation/saturation observed on sample

Many authors have studied the effect of drying and wetting cycles of COx claystone samples. Sample are subjected to air with a control Relative Humidity and mass or/and strain changes are measured. Some devices rely on a static atmosphere with saline solution [10-12], other used complex system with a steam generator and a heating channel, in which air is blown through the chamber [13].

Guillon et al [10] have performed static atmosphere drying tests which highlighted the HM coupling and mechanical anisotropy of the samples. Both wetting and drying paths were explored, allowing the potential hysteretic behaviour of the samples. During imbibition, the swelling of the sample is mainly achieved by the interaction of water with swelling clay sheets (illite/smectite interstratified, see [14]). The opening of some cracks can also be responsible for the dilation of the sample.

On the drying path, water is removed from the clay minerals that shrink. As the material progressively dehydrates, water menisci form in the porous space. These menisci strengthen the cohesion between grains and improve the apparent stiffness of the rock [15, 11]. This issue is highlighted by triaxial tests that were performed at the end of the drying tests or in other study. Zhang et al [16] performed micro-indentation and mini-compression tests on the COx claystone samples (11 mm× 22 mm) under different values of relative humidity.

The choice of sample size was justified by the fact that the sample should be large enough with respect to characteristic size of heterogeneities (mineral grains and bedding planes) and reasonably small in order to get uniform distribution of water saturation. They found that the mechanical properties of the claystone are strongly influenced by water saturation and structural anisotropy. The elastic modulus in the normal orientation to bedding planes is smaller than that in the parallel orientation. The deformation at failure state is larger in the perpendicular orientation than that in the parallel one due to progressive compaction of bedding planes. The elastic modulus and failure stress increase with desaturation of material.

At a smaller scale, Wang et al [17] also studied the evolution of the COx claystone under hydric cycles using techniques based on the combination of environmental scanning electron microscope (ESEM) and digital image correlation (DIC) [11], in order to quantify local strain field. The observation is carried out on zones of several hundred micrometers, so the evolution of such material under hydric loadings can be studied at the scale of inclusion-matrix composite. A heterogeneous strain field is evidenced at microscale during wetting. Nonlinear deformation is observed at high relative humidity (RH) which is related not only to damage, but also to the nonlinear swelling of the clay mineral itself, controlled by different local mechanisms depending on relative humidity. This sensitivity to variations in water content leads to enhanced variations of mechanical parameters in response to water saturation.

Among many factors related to desaturation and resaturation process, the suction plays an essential role due to the small size of claystone's pores (Figure 1). At mesoscopic scale, the suction generates not only an overall confining effect but also compaction or swelling of bedding planes. Such effects of water content are related to the modification of microstructure in clayey rocks [7]. Drying and wetting processes modify the distance between clay platelets, leading to modification of the mechanical properties of clay aggregates.

Zhang and Rothfuchs [18] performed creep test on COx claystone. **Figure 2** compares the creep curves of the specimens loaded parallel and perpendicular to the bedding plane. The total deformation perpendicular to the bedding plane is larger than that parallel to the bedding. However, the pure creep strains and the creep rates are not significantly dependent on the loading direction. In the last creep phase at 15 MPa, two initially saturated specimens were dried by exposing them to room air. The desaturation turned off creep rate, and even caused a significant shrinkage of 0.3%, independent of the loading direction to the bedding.

The question is how all those processes observed at sample scale will interact and affect the mechanical behavior of a gallery? Are those processes will just appear at the gallery wall or reach the rock mass deeper? Most of the experiment on desaturation/saturation have been performed on intact rock samples, also in situ at the main level of the MHM URL, Armand et al [4] show that excavation work induced a large fractures network depending of the drift orientation (see Section 4.5)? What will be the effect of desaturation/saturation on the fractured rock at the drift wall? A specific experiment, called Saturation Damaged Zone (SDZ), has been emplaced in 2009 at the main level of the MHM URL to try to better understand what really happened at this scale.

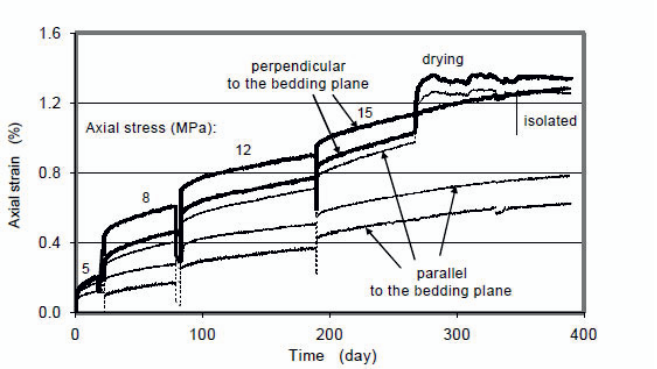

Figure 2. Effect of desaturation on creep test [18].

4 In situ experiment SDZ

4.1 Objectives

The objective of the SDZ experimentation is to study the effect of desaturation and saturation generated by the ventilation of galleries over the excavation damaged zone (EDZ). In this experiment (Figure 3), it is thus issue of:

• Measure changes in water saturation profiles in COx claystone around a drift under controlled ventilation conditions (temperature and relative humidity) over drying / wetting cycles;

• Characterize the EDZ and its development around a drift under controlled ventilation conditions (opening and closing of cracks initially present in COx claystone, appearance of new cracks, cracks connectivity ...);

• Characterize the mechanical evolution of a gallery subject to cycles of drying/wetting (deformation, convergence).

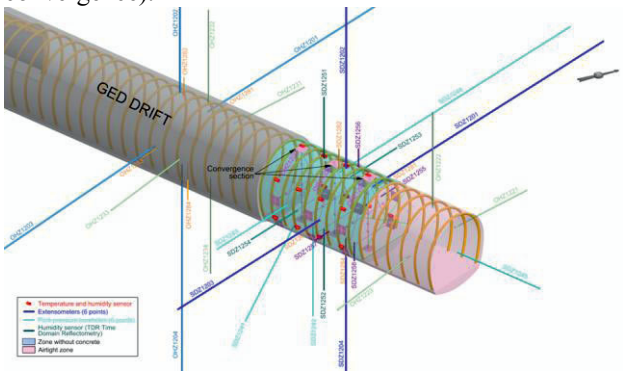

Figure 3. 3D view of dedicated instrumentations to the SDZ experimentation.

4.2 Experimental setup

The area dedicated to the SDZ experimentation (SDZ area) corresponds to the extremity of the GED drift parallel to the minor horizontal stress (σ_h). This area includes an airlock of 2 m long, an experimental area without coating of 7.2 m long (Zone 1) and a sealed area of 5 m long (Zone 2). The positioning of these areas

dedicated to SDZ experimentation is shown in Figure 4. The part of the GED drift forward the SDZ area (Zone 1 and Zone 2) is called in the paper Zone 0. The airlock doors are supposed airtight and waterproof.

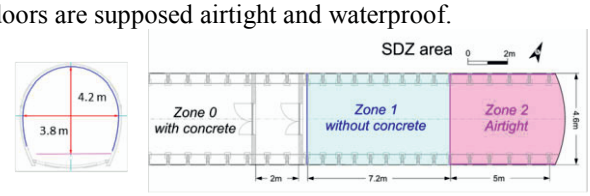

Figure 4. 2D view of SDZ area in the GED drift.

The excavation of the SDZ area took place from 12/01/2008 to 01/23/2009 (2 months). This period includes a stop work between 12/18/2008 and 01/05/2009. The floor of this area was sunk about 2 weeks after the end of the excavation. The ground support of Zones 0, 1 and 2 is ensured by a HA25 radial bolting (resin over their entire length) and sliding arches spaced 1 m in Zone 0 and 0.8 m in the SDZ area. The contact between the arches and the rocks is provided with a cement-filled Bulflex. Compressible slims are used to make the junction between the slab and the side elements of the arches. In the Zones 0 and 2, a wire mesh and fiber shotcrete 20~30 cm thick are set wall. The slab is 43 cm thick concrete. The theoretical final section of the Zones 0, 1 and 2 after excavation is identical, see Figure 4; the excavated diameter is 4.40 m. In Zone 2 assumed waterproof, a geotextile membrane and a heat-sealed plastic entirely cover the concrete. The Zone 1 is not coated and considered the main area of study.

The ventilation system dedicated to the SDZ experimentation was installed between July and August 2009. The regulation of air relative humidity (RH) and temperature is achieved through a cold battery, air heaters and steam humidifier. Several ventilation operation tests were conducted during September and October 2009. Four dates are important in the analysis of this experiment:

• 09/14/2009: closures airlock doors, no ventilation control,
• 09/01/2011: change of ventilation in the GED gallery,
• 10/03/2011: Start control of ventilation at SDZ area (RH = 30%, T = 23°C),
• 07/09/2013: change of relative humidity (RH = 60%, T = 23°C).

4.3 Main instrumentations

To achieve the above-mentioned objectives, several measures were carried out on geological, geomechanical, hydraulic and climatic aims. However, there are two major families of instrumentations: those carried out into the gallery and those carried out in the surrounding rock mass. Figure 3 shows the implementation of both families of instrumentations in the SDZ area.

Into the gallery

• arches sliding measurement by potentiometric displacement sensor,
• apparent cracks evolution measurements by potentiometric displacement sensor,
• hydrogeological test to measure hydraulic conductivities and permeabilities,
• geological survey of the front face and walls during excavation,
• climate sensors (relative humidity, temperature and air velocity),
• convergence-measuring gauge (with studs and rods);

In the surrounding rock mass

• geological survey on cored boreholes and front face (cracks analysis, core water content, mineralogy, calcimetry …),
• boreholes extensometers (single-point and multipoint) to capture rock displacement,
• boreholes pore pressures and permeability measurements,
• boreholes for TDR measurement of the saturation of the rock mass (water content),
• boreholes equipped with FD probes for measuring volumetric water content.

Thereafter the analysis will focus on the long-term behavior of a controlled ventilation gallery in the MHM URL.

4.4 Ventilation of the SDZ area

The measurements of the temperature and relative humidity at the inlet and at the outlet of Zone 1 are compared to those recorded in the Zone 0 in Figure 5. The four key dates are shown with the curves (dashed lines). This reflects that it is difficult to maintain a strictly constant temperature and relative humidity in the gallery. Seasonal variations are observed on Zone 0 measurements. At the scale of a circular section, a gradient, although small is always observed between ceiling and floor of the gallery.

Before closing airlock doors, many fluctuations were recorded on measurements. After closing the airlock, measured daily variations correspond to the fact that the drift ventilation retransmits external thermal fluctuations meaning a likely connection between the Zone 0 and the SDZ area. The temperature is high because the lighting lamps remained lit in this period. It is also observed on each circular section, of the Zone 1, an increasing thermal gradient from the ground to the roof. This thermal gradient is between 1°C and 1.5°C.

The set of Relative Humidity measurements presents similar behavior over the observation period. Both levels of 30% RH and 60% RH are visible throughout the Zone 1. It is also observed on each circular portion of the Zone 1, a decreasing gradient of moisture from floor to roof. This gradient is of the order of 4% and is also favored by the position of the arrival of moist air. The trend of rising relative humidity corresponds to the gradual re-saturation of air and probably reflects the efficiency of the isolation of the SDZ area from the rest of the GED gallery. Recent years, the ventilation of the SDZ facility loses its efficiency.

The SDZ area is 12.5 m long and the air flow is not laminar. Despite the position of a sensor inlet and outlet of the cooling unit, it is very difficult to make a precise assessment of the ventilation. Borehole temperature measurements in the first meters of Zone 2 (supposed sealed) teaches us that it is not possible to seal a portion of gallery as there is a connected fractures network.

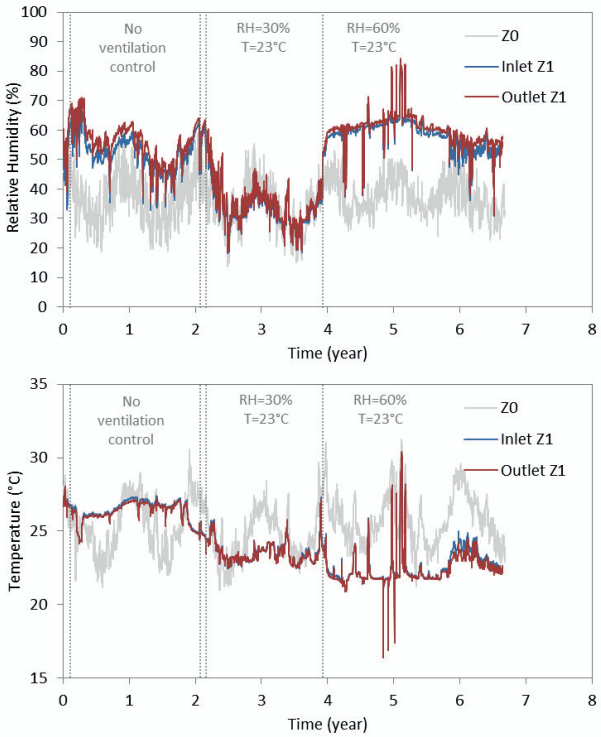

Figure 5. Average relative humidity and temperature in the Zone 0 (Z0) and Zone 1 (inlet Z1 and outlet Z1).

4.5 Excavation induced fracture network

An important characterization investigation of excavation-induced fracture network around openings has been conducted at the main level of Meuse/Haute-Marne URL by structural analysis of the front face and walls, the analysis of cores and resin impregnated cores [19].

Armand et al. [4] described the induced fractures network observed at the main level of the URL. Drift excavations exhibit extensional (mode I) and shear (mode II) fractures that were not observed in drifts at the –445 m level. Spalling is not the prevailing mechanism of failure due to the high-level mean stress compared to the Callovo-Oxfordian claystone strength. Shear failure seems to occur first from the excavation front face. Shear bands have been observed by the resin impregnation method at smaller scale confirming the shear failure mechanism. Armand et al. [20] showed that the fracture pattern and extent depend on the drift orientation versus the state of in situ stress. The maximum extent of fracture zones in different drifts can be summarized as follows:

(1) Drifts parallel to σ_H: the extensional and shear fractures are observed 0.4 and one diameter from the wall, respectively.

(2) At the floor and ceiling, shear and extensional fracture zones are mixed up to 0.15 diameter.

(3) Drifts parallel to σ_h: the extensional and shear fractures are observed up to 0.5 and one diameter respectively, at the roof and the ceiling. At the wall, shear and extensional fracture zones are mixed up to 0.2 diameter.

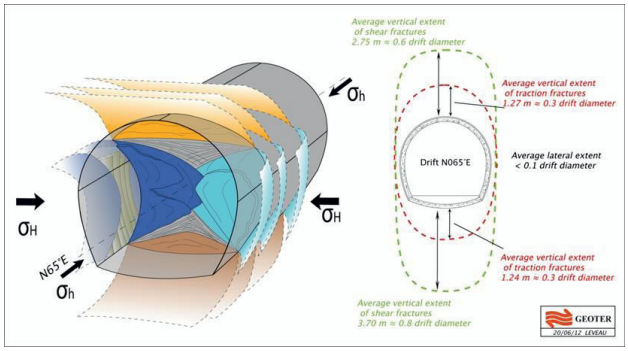

Figure 6. Conceptual model of the induced fractures network around a drift parallel to the horizontal major stress [4].

Figure 6 illustrates the model proposed to represent the fracture networks for drifts parallel to the minor horizontal principal stress, and Table 1 gives the extent of the different types of fracture zones for both orientations. Geological survey on cored borehole in the SDZ area confirms that the excavation induced fractures network follow the model given by Armand et al [4].

The area with unloading fractures (mode I) exhibits the highest hydraulic conductivity up to 10^{-10} m/s. Those high values are due to the fracture transmissivity and not the permeability of the rock matrix. Farther from the wall, the shear fractures exhibit low transmissivity, which did not affect considerably the average hydraulic conductivity. We can distinguish two zones: one with extensional and shear fractures which form a connected fractures network with potentially high transmissivity; one deeper from the gallery wall, where just remains some shear fractures or any (depending gallery orientation) with a slight decreasing hydraulic conductivity gradient to the pristine rock mass.

Table 1. Extent of shear and extensional fractures around drift at the main level of the URL.

Drift Orientation		Extensional fractures extent (*D*)			Shear fractures extent (*D*)		
		Min.	Ave.	Max.	Min.	Ave.	Max.
N65 // σ_h	C	0.2	0.3	0.4	0.5	0.6	0.8
	W	0.1	0.1	0.2	-	-	-
	F	0.2	0.4	0.5	0.8	0.8	1.1
N155 // σ_H	C	-	0.1	0.15	-	-	-
	W	0.01	0.2	0.4	0.7	0.8	1.0
	F	-	0.1	0.15	-	-	-

Note: D: is the drift's diameter;
C: ceiling;
W: wall;
F: floor;
'-' means no extent further the extensional fractures.

The extent of the fractured zone has been followed during time over a period of nearly 10 years for the older

gallery at the MHM URL. No significant change has been noticed yet.

5 Main results

5.1 Convergence and deformation of the rock mass

In this section, an analysis of rock deformation and support loading is made on the basis of convergence rods and measurement sections (SMR) constituted of 8 boreholes extensometers including 4 single-point (1.2 m) and 4 multi-points (7 anchors spread over 20 and 30 m). To evaluate the effect of ventilation and coating, a comparison is made between SMR measurements at Zone 0 and that of SDZ area (Zone 1). Those two SMR are distant of 13 m. Single-point and multipoint extensometers are positioned at the same inter arch. The measurements presented are recorded between the head of the extensometer (considered the reference point) and anchors (7). The positive displacement represents an extension (convergence of the walls). The SMR of Zone 0 was set during excavation (1.5 m from the front) and SMR of Zone 1 have been put in place 149 days after the excavation. Arbitrarily, these measurements are compared from a time t = 0 corresponding to a time tracking commencing 450 days after the excavation of the concerned zone; either from 01/25/2010 for Zone 0 and from 04/15/2010 for Zone 1. This means that short term convergence or displacements due to the excavation are not included in this study.

In the SDZ area (Zone 1); convergence rods were installed in pairs (vertical and horizontal). Figure 7 shows the measurements obtained by the convergence of rods at 1.2 and 3.6 m door of the airlock (Zone 1). The most important displacements and convergence speeds are measured on the vertical rods. Note that, convergence speeds are equivalent in Zone 0 and Zone 1. The convergence report (C_v/C_h) measured on all sections of the GED gallery is greater than 4.

A comparison of the displacements measured in the first meter by single-point and multipoint extensometers is done on Figure 8. Positive displacements represent convergence and negative displacements represent shrinkage. In this case (small strain), shrinkage could depict the effect of rock desaturation. It is observed that changes in relative humidity directly affect the rock mass in a field close to the wall. Last Relative Humidity change contributed to accelerating the strain rates. Extension areas are localized in roof and floor. The magnitude of the vertical displacement is thus the most important.

Thereafter, a comparison is done between the multipoint extensometers of the two SMR in Zone 0 and Zone 1. For this purpose, it represents what happens in horizontal (Figure 9) and vertical (Figure 10) borehole.
It may be noted that:
• The increase in relative humidity has contributed to increase the strain rate in in the first meter of the wall (Figure 7, Figure 8) meaning that, creep of COx claystone is dependent of relative humidity. This effect is not preponderant beyond the first meter on vertical multipoint extensometers (Figure 9), certainly given the magnitude of the measured deformations.
• Conversely, climate variations in the SDZ area have no effect on the arch sliding measurements since the postponement of the rock mass applied stresses on the arches remain still too important. The change in the boundary condition of relative humidity at drift wall has negligible impact on the drift convergence.
• The type of coating (shotcrete 20-30 cm thick or any) does not present a significant impact on the hygrometric condition at drift wall. Sprayed concrete does not play a structural effect in this case; it serves to prevent the falling blocks.
• The relative displacements among the different anchors beyond 5 m depth are very low (negligible).
These observations are insufficient to determine, at this stage of the experiment, if the re-saturation of the rock mass generated swelling deformation under in situ confinement.

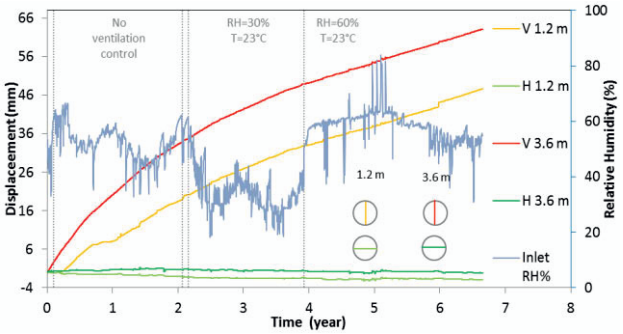

Figure 7. Inlet RH and convergence measurements in zone 1 of the area SDZ (Zone 1).

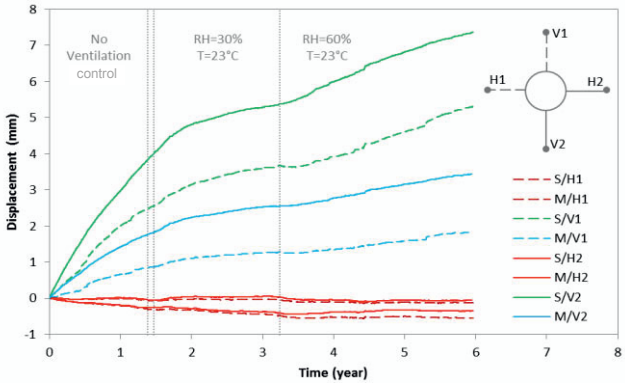

Figure 8. Displacement measurements comparison between single-point (S) and multipoint (M) borehole extensometers in the SDZ area (Zone 1).

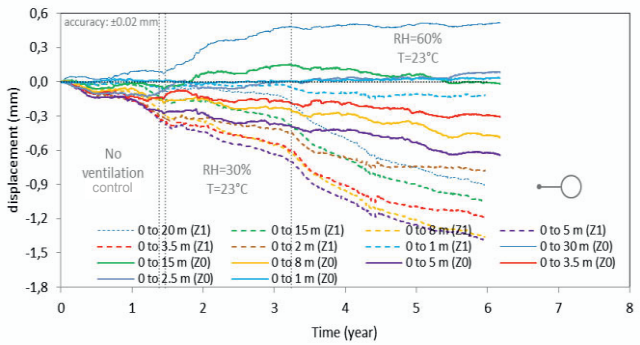

Figure 9. Evolution of displacement recorded by horizontal multipoint extensometers in Zone 0 and Zone 1, starting 450 days after excavation.

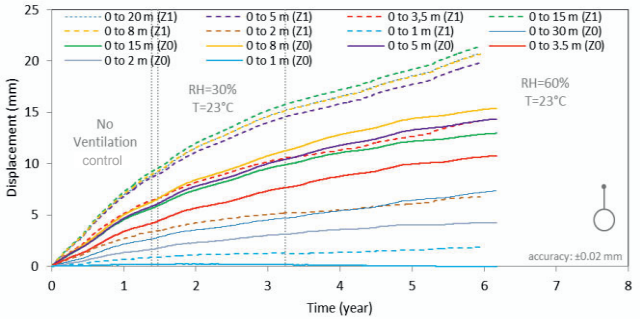

Figure 10. Evolution of displacement recorded by vertical multipoint extensometers in Zone 0 and Zone 1, starting 450 days after excavation.

5.2 Pore pressure and permeability measurements

In this section, the evolution of pore pressure is assessed at 3 m and 6 m (Figure 11) from drift wall through horizontal and vertical borehole. Pore pressure at this level (-490 m) is around 47 bar [20]. These figures show that the temperature fluctuations have a direct impact on pore pressures changes in the rock mass and thus its volumetric strain. Observed peaks on Figure 11 represent hydraulic tests to determine permeability. In long-term, no difference is observed at 3 m from drift wall on measurements between Zone 1 and Zone 2 (sealed area or not) on pore pressure measurements. This means that there is no difference between boundary conditions (bare / coated / waterproof wall). The sealing wall does not preclude the connectivity of the fracture network in the side wall. Ahead of the front, pore pressures at 3 m and 6 m remain high despite the extensive fracturing certainly because of the increase in vertical stress due to excavation. Pore pressures continue to decline over time (diffusive phenomenon).

Permeability measurements were performed (between 2009 and 2014) through gas and/or hydraulic tests. The aims were to assess the EDZ hydraulic conductivity with time and the degree of saturation of COx claystone [21, 22]. The results of these campaigns show that the permeability of the rock into the damaged area does not evolve much post excavation (Figure 12). Note that clay formations in their natural state generally have a very low hydraulic conductivity (~10^{-13} m/s).

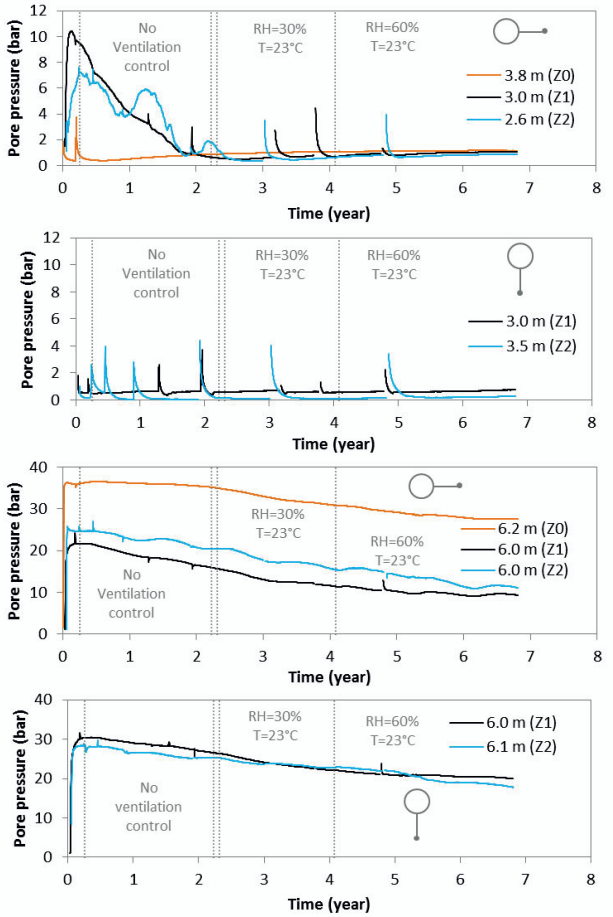

Figure 11. Evolution of borehole pore pressure measurements at 3 m and 6 m deep in the Zone 0, 1 and 2.

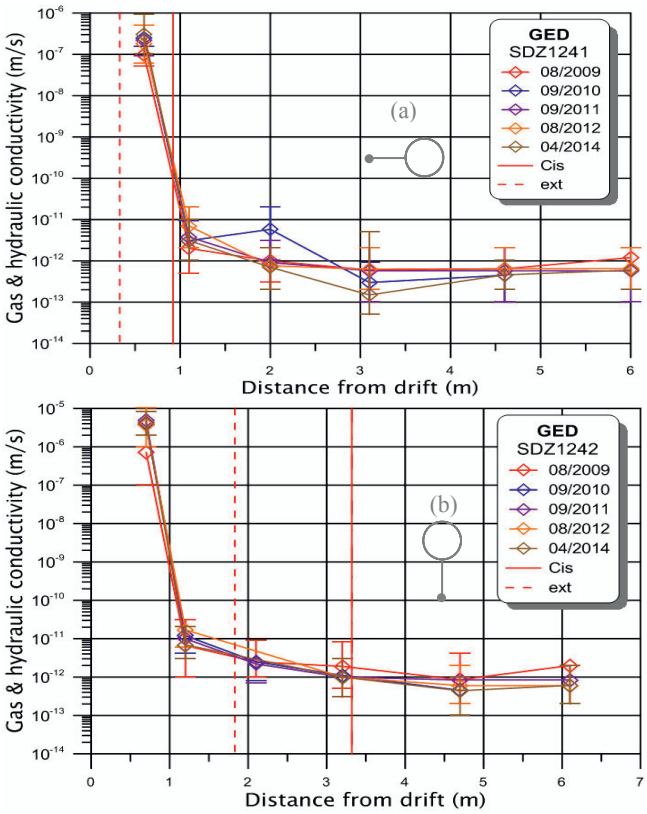

Figure 12. Permeability measurements in horizontal (a) and vertical borehole (b) in SDZ area (Zone 1).

For all boreholes, permeability values in excess of 3.0 m away from the gallery are characteristic of undisturbed COx claystone, or micro-cracks close to the limit with a undisturbed COx claystone. Permeability values characteristic of a micro-fractured COx claystone were observed between 1 and 3 m from wall. Permeability values obtained to the nearest interval of the gallery (~0.6 m) are characteristic of an unsaturated fractured zone (tire testing). Saturated intervals closest to the gallery mostly indicate pressures near or below atmospheric pressure, and the high specific storage coefficients.

5.3 Water content and saturation of the rock mass

In this part, rock mass saturation profile is evaluated in the first meters from the wall through horizontal and vertical boreholes. For this purpose, gravimetric (Figure 14-a) and boreholes water content measurements (Figure 13 and Figure 15) are carried out.

In Figure 14-a, an increase in gravimetric water content measurement is observed in the first meters from the wall, subsequently the water content is between 7 and 8% over 2 and 7 m. Geological survey were carried out between 2008 and 2015 on annual basis. The change in mineralogy at the cores sample scale justifies this value range. This measure is similar to that measured in other galleries of the underground laboratory. An extension of the low water content area with time is not observed. The changes in relative humidity do not affect the rock saturation measurements in the near field of the wall.

The TDR (Time Domain Reflectometry) packer system shown in Figure 13 is composed of a dual shutter completion which defines six measurement points of the rock mass water content. The determination of the water content using TDR is based on the principle that the relative dielectric number of water is much larger than that of other rock constituents (solid, air). The dielectric number can be measured by determining the propagation velocity of an electromagnetic wave along uncoated metallic waveguides. Figure 14-b highlights a desaturation of the wall even before the installation of the controlled ventilation facility in the SDZ area. One of the main difficulties that may arise from using the TDR method is to ensure optimal contact between the probe and the measuring medium (rock mass). The results of these sensors are difficult to interpret after a year of measurement. It seems that complete desaturation of the rock/sensor interface (opening of the interface) lasted about 2 years or not proper functioning. This shows that it is very difficult to make a continuous measurement of the rock mass water content. Desaturation is related to the fracture zone due to the extension. So, the reliable measurement between the two methods is gravimetric.

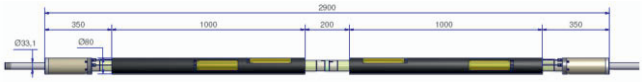

Figure 13. Layout of the TDR packer system

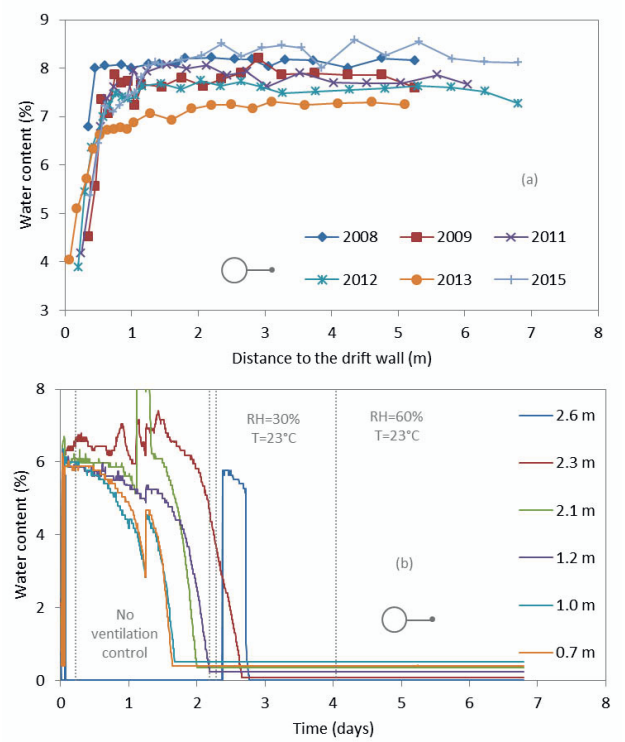

Figure 14. Gravimetric (a) and borehole (b) water content measurements in the SDZ area (Zone 1).

The volumetric water content is measured through FD probe by propagation over 100 mm of an electromagnetic field. FD probe is equipped with a completion, defining six measurement points in the surrounding rock mass (Figure 15). Results are given in Figure 16-a for a horizontal borehole and in Figure 16-b for a vertical borehole. This shows that, the volumetric water content measurements are not sensitive to relative humidity changes at drift wall. This observation is consistent with the gravimetric water content measurement shown on Figure 13-a.

Figure 15. Layout of FD probe (L=1,35 m, Φ=25 mm, 950 g).

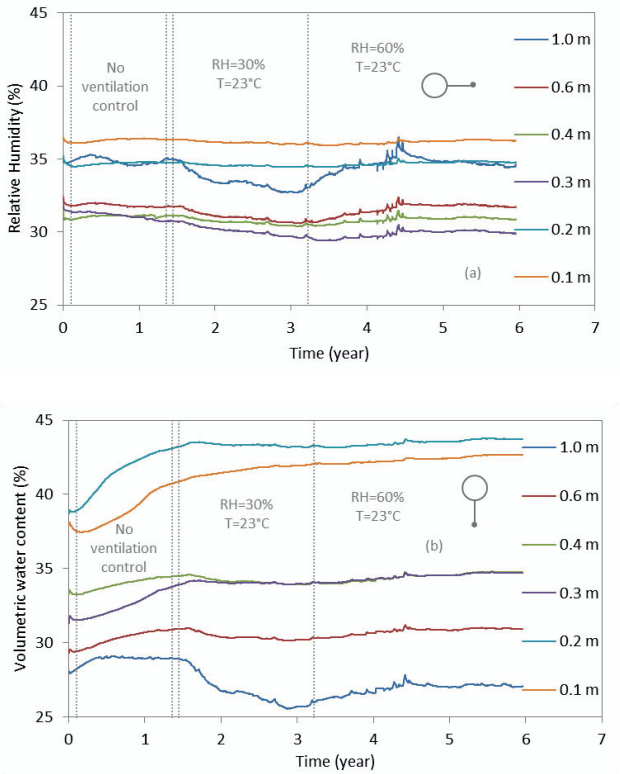

Figure 16. Volumetric water content changes in the rock in SDZ area (Zone 1).

5.4 Selected cracks evolution at drift wall

Crack development measurements are carried out by potentiometric displacement sensors also called fissurometers. These sensors are fixed on two ankles anchored on either side of the selected crack. Followed crack is chosen opportunistically. 2 types of cracks are selected: fractures generated by shearing (S) and extension (E). Figure 17 shows the data acquired from fissurometers since their installation. Positive displacements reflect the closing of the studied crack. It is observed that most fissurometers appears to have identical developments trends: decreasing slightly regardless of the type of cracks and, a very small opening. The closing rate observed at 30% RH is greater than that observed at 60% RH (very low). Most cracks therefore have almost stopped evolving since the last change of relative humidity. Only one tensile fracture continues to close.

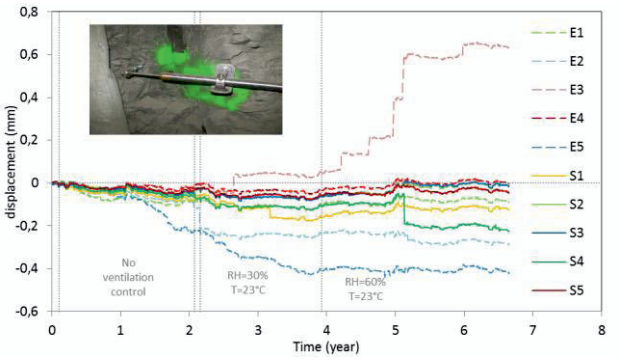

Figure 17. Measurements of cracks evolution at drift wall in the SDZ area (Zone 1).

6 Discussions

From experimental point of view, desaturation experiment on COx claystone at gallery scale remains challenging. In fact, desaturation or water content measurements are difficult in such rigid and low permeable media. The online measurements (TDR, volumetric water content) are not working properly and even failed. The TDR system was based on a packer system in order to get a good contact between the needles and the rock. At the beginning it seems to work but on larger time desaturation occurs or the system downward slide or failed. For the volumetric water content, evolution is somehow coherent with gravimetric water content evolution, but the initial gradient in the rock from the gallery wall is strange and need further analysis. Capacitive and psychrometric measurement hygrometers have been installed in cross section of the Ventilation Experiment (VE) at Mont Terri [23] and performed successfully. At MHM URL, doubt on those values remains. Due to the excavation induced fractures network, it could be possible that the highest water content is not the deepest in the rock wall due to the presence of connected fractures. Geoelectric measurements have been although used in VE experiment at Mont Terri (Mayor et al, 2007), but could not be used easily in the context of SDZ experiment due to the presence of metallic rock bolt necessary for the gallery support. The fact, that saturation degree in field remains uncertain to measure continuously in the gallery wall, makes interpretation of desaturation cycles more difficult. Better systems have to be developed to have more reliable data.

On the side wall, water content gradient is observed in the first meters from the wall and have not evolve since the excavation of the gallery despite low RH in the gallery air. The extent of the lower water content matches with the extent of the induced fracture zone with shear and extensional fractures. Nevertheless, a suction state develops up to a larger distance about 3 m from the wall for horizontal boreholes.

As the wall is highly fractured during the excavation, there is no evidence of desiccation cracks outbreak during the drying period as seen at Tournemire [3]. A slight opening of the excavation induced fractures is measured over 1.5 years under RH equal to 30 % and the increase of RH in the gallery air seems to interrupt this opening. In the surrounding rock mass the increase in RH has contributed to increase the strain rate in in the first meter of the wall, but deeper in rock mass no effect was observed. In the first meter, creep of COx claystone is dependent of relative humidity as demonstrate by Zhang & Rothfuchs [18] on samples.

Strain, permeability and pore pressure measurements give the same insight of a low impact of the desaturation included in the excavation induced fractures. Those results are in accordance with what has been observed during the VE experiment at Mont Terri even if the excavation induced fractures network is less developed at Mont Terri and nearly not existing around VE gallery. Mayor et al. [23] show that only very small shrinkages of the rock have been detected during the

desaturation period. Moreover they conclude that the thermal and hydraulic rock characteristics will not be practically affected by the ventilation except in a narrow ring around the drift (less than 30 cm for a gallery of 2.4 m diameter), where the degree of rock saturation can be lower than 98 %.

The excavation induced fractures are a major issue to understand desaturation around the GED. de La Vaissiere et al [24] have performed gas circulation tests at the wall of a drift parallel to the major stress (in this situation the excavation induced fractures network is mainly develop at the wall at the MHM URL, see section 4.5). These tests showed that fractures may be connected to one another and allow gas circulation only in the zone where extensional fractures are observed. We can assume that it is the case also along the GED gallery. Vinsot et al [25] tracked oxidation front defined as the set of deepest points away from the drift walls where oxidation reactions have occurred. The oxidized features encountered mainly consisted of weathered pyrite minerals associated with gypsum, as well as iron oxides and hydroxides and are analyzed on drill core. Finally, over 6.5 years, they found that the oxidation front has propagated deeper into the fractured zone and has developed in the shear zone. Nevertheless, all the oxidized features were encountered at less than 1.8 m from the drift walls, and none were found within the deepest part of the shear zone over the maximum lag time of the study (6.5 years). The evolution of the oxidation front over time implies that gas diffusion was facilitated in the shear fracture when compared to the pristine rock. Those chemical results underline the role of the fracture network which has to be considered in modelling in order to predict the gallery behavior during and after excavation.

Pardoen et al [26] shows that the fractures induced by excavation process in the gallery vicinity could be reproduced by shear banding, with strain localisation properly reproduced by means of a regularisation method. Taking into account intrinsic permeability evolution in the shear band conduct with localisation methods seems to be promising to better reproduced the behavior of GED gallery, with its anisotropy, its long-term evolution and the influence of desaturation.

7 Conclusions and perspectives

An in situ experiment, called SDZ, has been implemented at the main level of the MHM URL in order to characterize the influence of controlled ventilation in an experimental drift. The aim is to analyse the hydro-mechanical behaviour of the rock mass and the excavation damaged zone evolution. The desaturation process, the permeability and the deformation of the surrounding clay rock are most particularly studied during the tests. Relative humidity (of 30% then 60%) has been applied over a period of more than 4 years.

Effect of ventilation with dry air remains small and concentrated in the vicinity of the drift in the zone with shear and extensional fractures. The extent of the lower water content matches with the extent of the extensional fractures. Unfortunately, some of the online water content measurements failed or were uncertain which increases the difficulty of following of saturation field. Better systems have to be developed to have more reliable data. No evidence of desiccation cracks outbreak has been observed, but excavation induced fractures which are widespread at the drift wall show small opening during the driest phase. The opening tendency decreases with RH increase.

The experiment already provided inputs over 7 years of drying phase and will continue with an increase of relative humidity up to 90% to see if swelling occurs and the impact in the connected excavation induced fracture network. This increase of HR will represent the closing of the drift in the nuclear disposal with ventilation stop. In parallel, effort on modelling will be done through benchmark exercise in order to improve constitutive modelling of COx claysone behavior in unsaturated state.

References

1. J. Delay, A. Vinsot, J.-M. Krieguer, H. Rebours, G. Armand, Phys. Chem. Earth J., **32** (1/7), 2-18, (2007).
2. J.-M. Matray, S. Savoye, J. Cabrera, Eng. Geol. ,**90**, 1-16, (2007).
3. S. Hedan, A.-L. Fauchille, V. Valle, J. Cabrera, P. Cosenza, Int. J. Rock Mech. Min. Sci. **68**, 22-35, (2014).
4. G. Armand, F. Leveau, C. Nussbaum, R. de La Vaissiere, A. Noiret, D. Jaeggi, P. Landrein, C. Righini, Rock Mech. Rock Eng. **47**, Issue 1, 21-41 (2014).
5. C. Lerouge, S. Grangeon, E.C. Gaucher, C. Tournassat, P. Agrinier, C. Guerrot, D. Widory, C. Fléhoc, G. Wille, C. Ramboz, A. Vinsot, S. Buschaert,. Geochim. Cosmochim. Acta, 75, 2633-2663, (2011).
6. B. Yven, S. Sammartino, Y. Geraud, F. Homand, F. Villieras, Mémoires de la Société géologique de France **178**, 73-90, (2007).
7. J.-C. Robinet, P. Sardini, M. Siitari-Kauppi, D. Prêt, B. Yven, Sediment. Geol. **321**, 1-10, (2015).
8. J.-C. Robinet, P. Sardini, D. Coelho, J.-C. Parneix, D. Prêt, S. Sammartino, E. Boller, S. Altmann, Water Resour. Res. **48**, (2012).
9. Y. Song, C. Davy, D. Troadec, A.-M. Blanchenet, F. Skoczylas, J. Talandier, J.-C. Robinet, Mar. Petrol. Geol. **65**, 63-82, (2015).
10. T. Guillon, R. Giot, A. Giraud, G. Armand, Acta Geotech. **7**, 313-332, (2012).
11. M. Bornert, F. Valès, H. Gharbi, D. Nguyen Minh, Strain **46**, 33-46, (2010).
12. Q.T. Pham, F. Valès, L. Malinsky, D. Nguyen Minh, H. Gharbi, Phys. Chem. Earth J. **32**, 646-655, (2007).
13. P. Gerard, A. Leonard, J.P. Masekanya, R. Charlier, F. Collin, Int. J. Numer. Anal. Meth. Geomech. **34**, 1297-1320, (2010).
14. H.G. Montes, J. Duplay, L. Martinez, S. Escoffier, D. Rousset, Appl. Clay Sci. **25**, 187-194, (2004).
15. L. Dormieux, J. Sanahuja, S. Maghous, C R Mecanique 334:19-24, (2006).
16. F. Zhang, S.Y. Xie, D.W. Hu, J.F. Shao, B. Gatmiri, Appl. Clay Sci. **69**, 79-86, (2012).

17. L. Wang, M. Bornert, S. Chanchole, Poromechanics V, 1635-1643 (2013).
18. C.L. Zhang, T. Rothfuchs, Appl. Clay Sci., **26** (1-4), 325-336, (2004).
19. G. Armand, Y. Wileveau, J. Morel, M. Cruchaudet, H. Rebours, *Proc. 11th Congress of the International Society for Rock Mechanics*, Riberiro e Sousa, Olalla&Grossmann (eds), 33-36, (2007).
20. G. Armand, A. Noiret, J. Zghondi, D.M. Seyedi, Rock Mech. and Geotech. Eng. J. **5**, 221–230, (2013).
21. P. Bossart, P.M. Meier, A. Moeri, T. Trick, J.-C. Mayor, Eng. Geol., **66**, 19-38, (2002).
22. T. Fierz, M. Piedevache, J. Delay, G. Armand, J. Morel. *Proc. 7th International Symposium on Field Measurements in Geomechanics*, (2007).
23. J.C. Mayor, M. Velasco, J.L. García-Siñeriz, Phys Chem Earth J., **32**(8-14):616-628, (2007)
24. R. de La Vaissière, G. Armand, J. Talandier, J. Hydrol. 521, 141–156 (2015).
25. A. Vinsot, F. Leveau, A. Bouchet, A. Arnould, Clays in Natural and Engineered Barriers for radioactive Waste Confinement, **400**, 37, (2014).
26. B. Pardoen, S. Levasseur, F. Collin, Rock Mech. Rock Eng. **48**, 2, 691-714, (2015).